Electronic Supplementary Material (ESI) for Physical Chemistry Chemical Physics.

SUPPORTING INFORMATION

High-temperature molecular screening of hybrid polyOAPS-imide networks based on octa(aminophenyl)silsesquioxane for increased thermomechanical resistance

Sylvie Neyertz, Saman Salimi, Farzaneh Radmanesh, Nieck E. Benes and David Brown

1) ATOM-TYPES AND FORCE-FIELD PARAMETERS

The atom-types used for OAPS and the polyOAPS-imides are defined in Table S1. The atom-types and the parameters for the aliphatic POSS and polyPOSS-imides have been given previously.[1,2]

Table S1 Atom-types for all OAPS-based molecules

Atom-type	Description
Si	Silicon on siloxane cage
O	Oxygen on siloxane cage
Car	Aromatic carbon
Hcar	Hydrogen on aromatic carbon
Npri	Nitrogen on primary amine
Hnpri	Hydrogen on primary amine
Ckanhy	Ketone carbon on dianhydride
Okanhy	Ketone oxygen on dianhydride
Oanhy	Anhydride oxygen on dianhydride
Ckimide	Ketone carbon on polyOAPS-imide
Okimide	Ketone oxygen on polyOAPS-imide
Nimide	Imide nitrogen on polyOAPS-imide
C_1	$(CF_3)_2$-bearing carbon on 6FDA dianhydride and polyOAPS-imide
C_2	F_3-bearing carbon on 6FDA dianhydride and polyOAPS-imide
F	Fluorine on 6FDA dianhydride and polyOAPS-imide
Oether	Ether oxygen on ODPA dianhydride and polyOAPS-imide

The classical force-field used for the MD simulations in the *gmq* code[3] is given by Equation A:

$$U_{pot} = \sum_{\theta} U_{bend}(\theta) + \sum_{\tau} U_{tors}(\tau) + \sum_{i-planar} U_{oop}(i) + \sum_{(i,j)nb} U_{vdw}(r) + \sum_{(i,j)nb} U_{coul}(r) \qquad \text{(A)}$$

where the first three terms are referred to as the "bonded" potentials and the last two terms as the "nonbonded" potentiels. All bonds were kept rigid using the SHAKE algorithm.[4] The five terms in Equation A are detailed hereafter.

The angle-bending deformations are described by a harmonic function in the cosine of the bond angles θ:

$$U_{bend}(\theta) = \frac{k_{\theta}}{2}\left(\cos\theta - \cos\theta_0\right)^2 \qquad \text{(B)}$$

where k_{θ} is a constant determining the flexibility of the angle and θ_0 is the equilibrium bond angle. No specific angle-bending potentials were used to restrict the Si-O-Si and O-Si-O angles, since the combination of the rigid Si-O bonds and the non-bonded U_{vdw} and U_{coul} terms were sufficient to maintain the geometry of the cage. To ensure the equipartition of kinetic energy, the high-frequency motions of hydrogens in CH_2, CH and NH_2 groups were removed using special constraints.[4,5] The equilibrium Hnpri-Npri-Hnpri and Car-Npri-Hnpri angles were set to 112.2 and 115.4 degrees, respectively.

The torsional motions around the dihedral angles τ are represented by a third-order polynomial in $\cos\tau$:

$$U_{tors}(\tau) = \sum_{n=0}^{3} a_n \cos^n \tau \qquad \text{(C)}$$

with the dihedral angle τ varying from -180° to +180°, $\tau = 0°$ being the *trans* conformation and a_n being the torsional coefficients. The wild card denotes any atom-type, except when the coefficients for a specific dihedral are defined elsewhere. It should be noted that the *-Si-Car-* dihedral potential had to be represented by a sixth-order polynomial, so the sum in Eq. C runs from $n = 0$ to 6 for that specific angle.

The out-of-plane term, keeps sp^2 structures planar by using a harmonic function in the perpendicular distance d from the central atom i to the plane defined by its three attached atoms with k_{oop} being the force constant:

$$U_{oop}(i) = \frac{k_{oop}}{2} d^2 \qquad \text{(D)}$$

A coplanar vector bisector constraint designed to remove the degrees of freedom of the Hcar atoms in the aromatic Car-Hcar groups is applied as a special form of the out-of-plane terms.[3,4]

The "nonbonded" excluded-volume van der Waals and electrostatic potentials, which depend on the distance r between two interacting sites, were applied to all atom pairs situated either on the same molecule (but separated by more than two bonds if the intervening angles are subject to the bending potential or by more than one bond otherwise) or on two different molecules. The van der Waals interactions are described in Equation A by the 12-6 Lennard-Jones form:

$$U_{vdw}(r) = U_{LJ}(r) = 4\varepsilon\left(\left(\frac{\sigma}{r}\right)^{12} - \left(\frac{\sigma}{r}\right)^{6}\right) \tag{E}$$

where ε is the well-depth of the potential and σ is the distance at which the potential is zero. The cross-terms for unlike-atom pairs are obtained from the standard combination rules[6] given by:

$$\sigma_{ij} = \frac{\sigma_{ii} + \sigma_{jj}}{2} \qquad \varepsilon_{ij} = \sqrt{\left(\varepsilon_{ii} \times \varepsilon_{jj}\right)} \tag{F}$$

The van der Waals cutoff was set to 12 Å and long-range corrections to the energy and the pressure were implemented.[6]

The last term of Equation A accounts for the Coulombic interactions with q_i and q_j being the partial charges on atoms i and j respectively, and ε_0 being the vacuum permittivity:

$$U_{coul}(r) = \frac{q_i q_j}{4\pi\ \varepsilon_0\ r} \tag{G}$$

This long-range electrostatic potential was calculated using the Ewald summation method,[7-9] with a real space cutoff R_c of 12 Å, the reciprocal space sum K_{max} being typically equal to 12-14 and the separation parameter α being typically equal to 0.19-0.23 depending on the systems under study.

The average bond-lengths b_0, bond-angles θ_0 and partial charges q_i/e were obtained by performing Density Functional Theory (DFT) optimizations on representative fragments of the molecules under study in vacuum with the Gaussian09 code[10] at the B3LYP/6-31G** level. The partial charges were then extracted by an ESP-fitting procedure[11,12] and symmetrized with respect to the nature and the position of the atoms. The partial charges on the unreacted -NH_2 arms of the cross-linked OAPS were kept identical to those in the pure OAPS, since they were very close in the DFT-optimised systems.

Similarly, the *-Si-Car-* and the *-Npri-Car-* torsional potentials were obtained from the DFT optimizations by calculating the total energy of the *para*OAPS molecule as a function of the rotation around these specific bonds, and adapting it to the form of the present classical force-field (Eq. A). Because of the symmetry of the tetrahedral Si and the planar Car, a sixth-order polynomial in the cosine of the torsional angle had to be used in place of the third-order polynomial of Eq. C for the *-Si-Car* potential. Only its a_0 and a_6 (indicated by a hash sign # in Table S3) coefficients were non-zero. On the other hand, the *-Npri-Car-* torsional potential could be described by Eq. C.

The other force-field parameters were adapted from the literature.[13-15] As used elsewhere for aromatic siloxanes,[16,17] the O-Si-Car bending constant was chosen equal to the corresponding one for Si and aliphatic C.[14] All parameters used in Equation A are given in Tables S2-S3 and in Fig. S1.

Table S2 Force-field parameters for the bonds, the bending (Eq. B) and the out-of-plane (Eq. D) potentials. The symbols - show that no parameters are defined for these interactions.

Bond types	b_0 / Å	**Bond-angle type**	θ_0 / deg	k_θ / kJ.mol^{-1}	**Out-of-plane atom**	k_{oop} / kg s^{-2}
Si-O	1.65	O-Si-O	109.0	-	Car	667
Si-Car	1.85	Si-O-Si	148.8	-	Ckanhy	667
Car-Car	1.40	O-Si-Car	109.9	477.8	Ckimide	667
Car-Npri	1.39	Si-Car-Car	120.9	879.1	Nimide	167
Car-Nimide	1.43	Car-Car-Car	120.0	879.1		
Car-Ckanhy	1.49	Car-Car-Npri	120.6	1465.1		
Car-Ckimide	1.49	Car-Car-Nimide	119.6	2270.9		
Car-Oether	1.38	Car-Car-Ckanhy	119.0	879.1		
Car-C1	1.55	Car-Car-Ckimide	119.1	879.1		
Car-Hcar	1.08	Car-Car-Oether	119.1	2270.9		
Ckanhy-Okanhy	1.20	Car-Car-C$_1$	120.2	879.1		
Ckanhy-Oanhy	1.40	Car-Car-Hcar	120.1	879.1		
Ckimide-Okimide	1.21	Car-Nimide-Ckimide	124.2	1904.6		
Ckimide-Nimide	1.42	Car-Ckanhy-Okanhy	130.3	952.3		
Npri-Hnpri	1.01	Car-Ckanhy-Oanhy	107.1	1098.8		
C$_1$-C$_2$	1.56	Car-Ckimide-Okimide	128.2	952.3		
C$_2$-F	1.35	Car-Ckimide-Nimide	105.7	1465.1		
		Car-Oether-Car	121.5	622.2		
		Car-C$_1$-Car	111.4	556.5		
		Car-C$_1$-C$_2$	109.4	742.0		
		Okanhy-Ckanhy-Oanhy	122.6	1098.8		
		Ckanhy-Oanhy-Ckanhy	110.4	622.2		
		Okimide-Ckimide-Nimide	126.1	1171.7		
		Ckimide-Nimide-Ckimide	111.5	659.3		
		C$_2$-C$_1$-C$_2$	108.0	742.0		
		C$_1$-C$_2$-F	111.5	618.3		
		F-C$_2$-F	107.4	1236.6		

Table S3 Force-field parameters for the torsional (Eq. C) and van der Waals (Eq. E) potentials. The symbols * denote a wild card. See text for detail for the hash sign #

Dihedral type	a_0 / kJ.mol^{-1}	a_1 / kJ.mol^{-1}	a_2 / kJ.mol^{-1}	a_3 or $a_6^{\#}$/ kJ.mol^{-1}	Like-atom pair	σ_{ii} / Å	ε_{ii}/k_B / K
-Si-Car-	-0.135	0	0	$0.480^{\#}$	Si...Si	3.385	294.38
-Car-Car -	16.736	0	-16.736	0	O...O	2.955	102.15
-Car-Npri-	11.380	0	-11.380	0	Car...Car	3.029	53.84
-Car-Nimide-	13.389	0	-13.389	0	Ckanhy...Ckanhy	3.029	53.84
-Car-Ckanhy-	13.389	0	-13.389	0	Ckimide...Ckimide	3.029	53.84
-Car-Ckimide-	13.389	0	-13.389	0	C_1...C_1	3.029	53.84
-Car-Oether-	10.041	0	-10.041	0	C_2...C_2	3.029	53.84
-Car-C_1-	0.502	-1.506	0	2.008	Oanhy...Oanhy	2.708	58.37
-Ckanhy-Oanhy-	48.534	0	-48.534	0	Okanhy...Okanhy	2.708	58.37
-Ckimide-Nimide-	54.057	0	-54.057	0	Okimide...Okimide	2.708	58.37
*-C_1-C_2-F	0.837	2.510	0	-3.347	Oether...Oether	2.708	58.37
					Npri...Npri	2.762	47.81
					Nimide...Nimide	2.762	47.81
					Hcar...Hcar	2.673	21.14
					Hnpri...Hnpri	2.673	21.14
					F...F	2.619	54.85

***meta*OAPS**

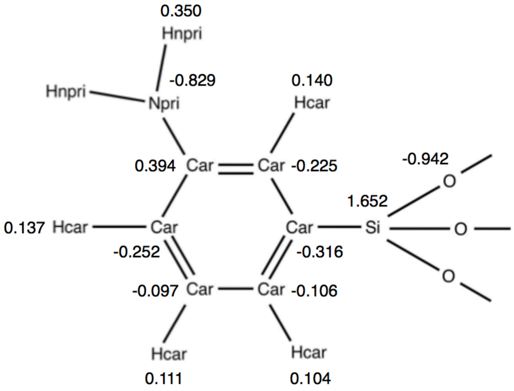

***para*OAPS**

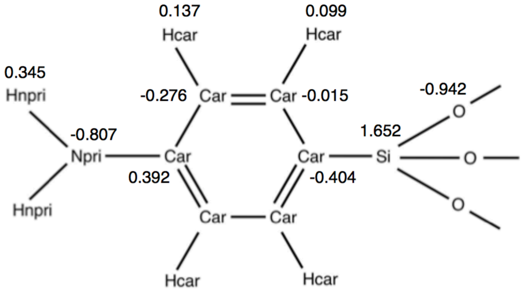

***ortho*OAPS**

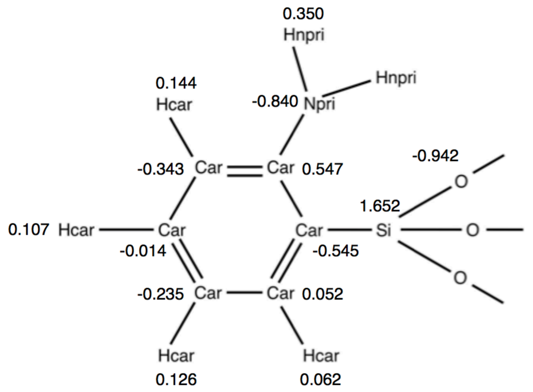

6FDA

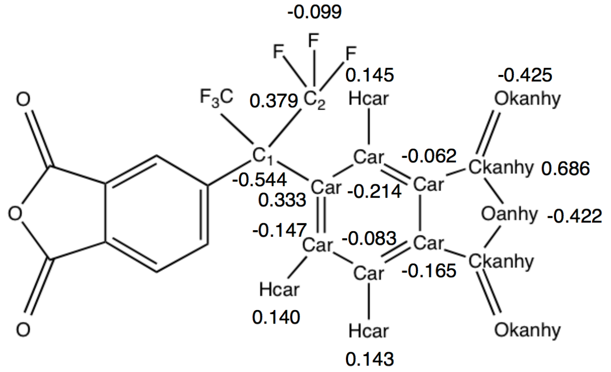

PMDA

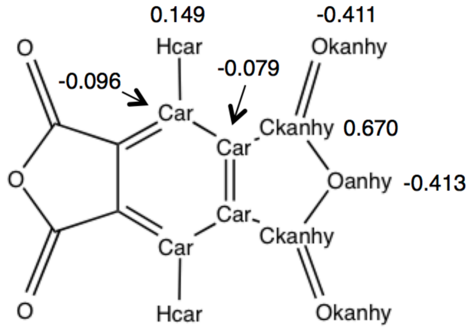

ODPA

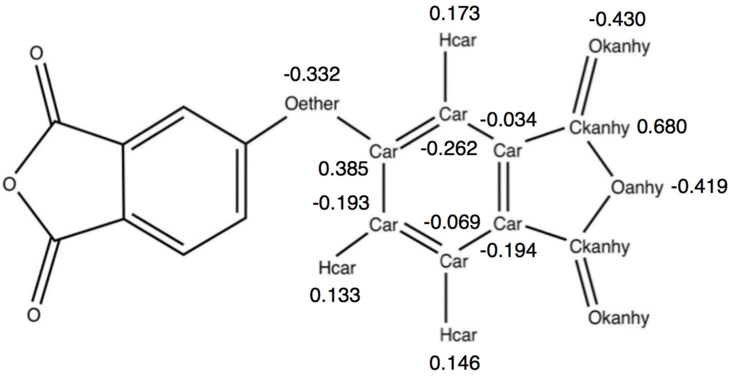

poly*meta*OAPS-6FDA

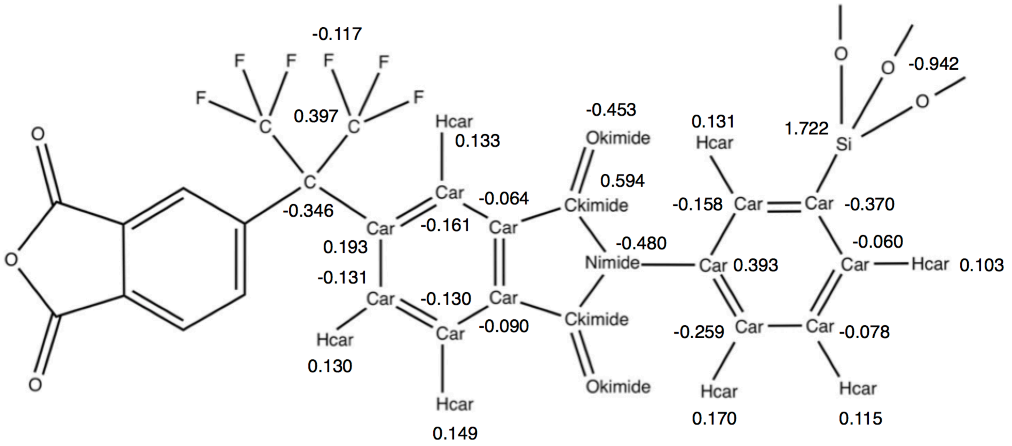

poly*para*OAPS-6FDA

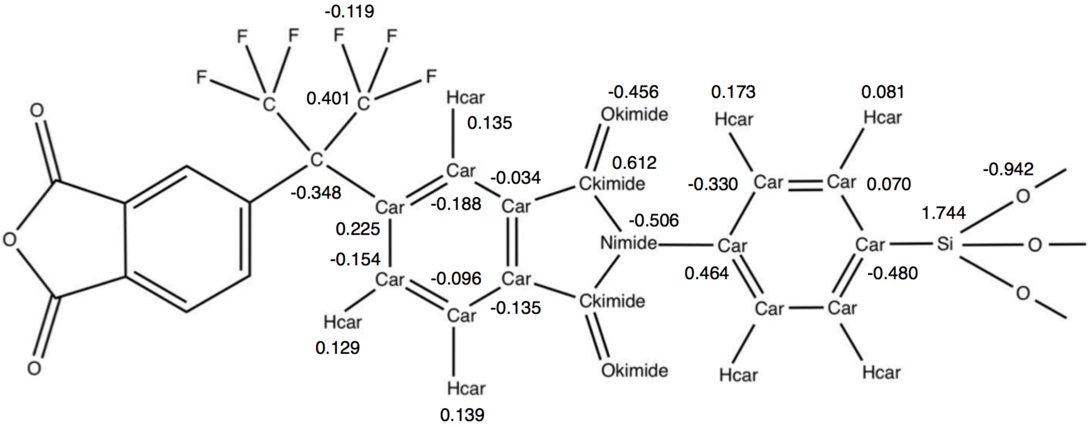

poly*ortho*OAPS-6FDA

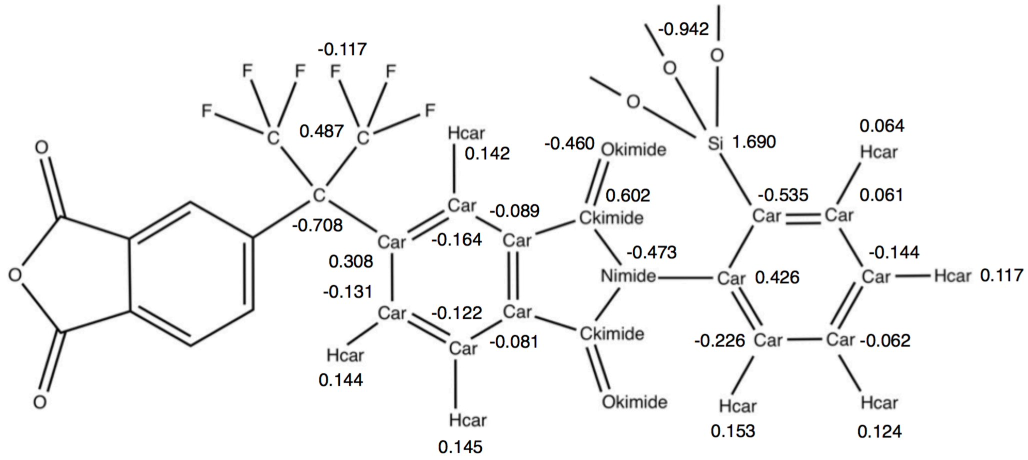

poly*meta*OAPS-PMDA

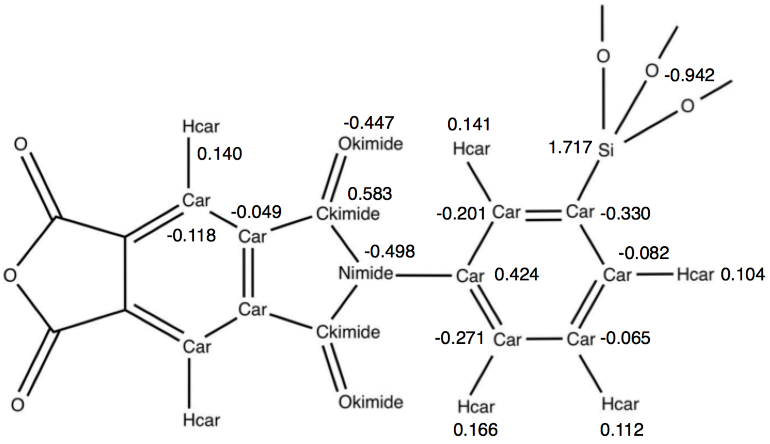

poly*para*OAPS-PMDA

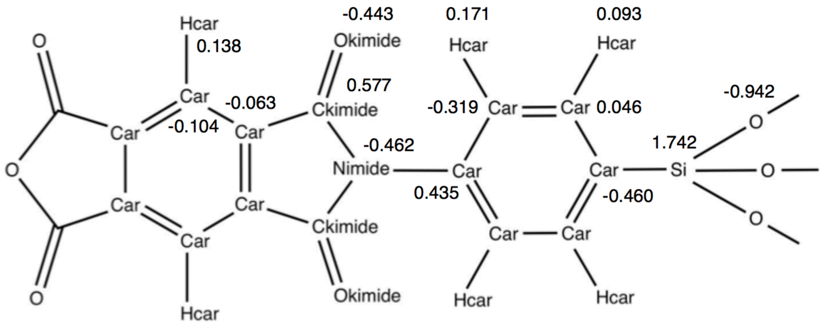

poly*ortho*OAPS-PMDA

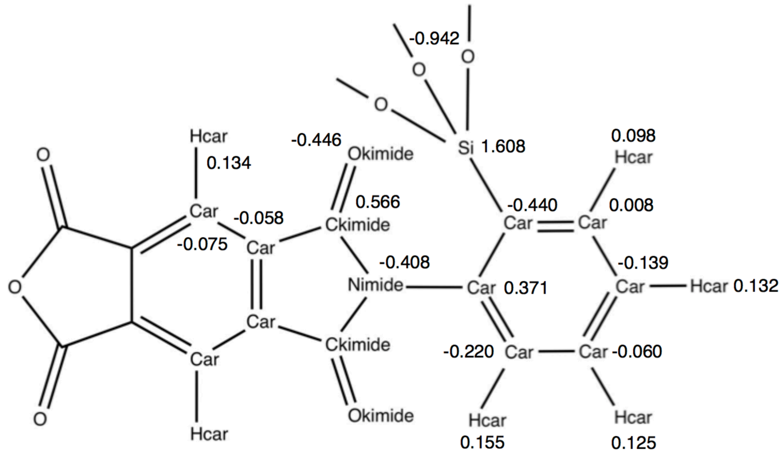

poly*meta*OAPS-ODPA

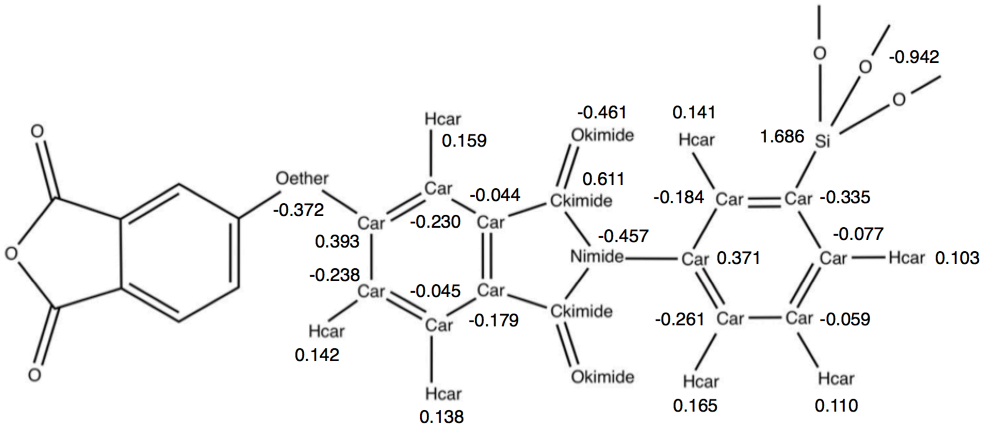

poly*para*OAPS-ODPA

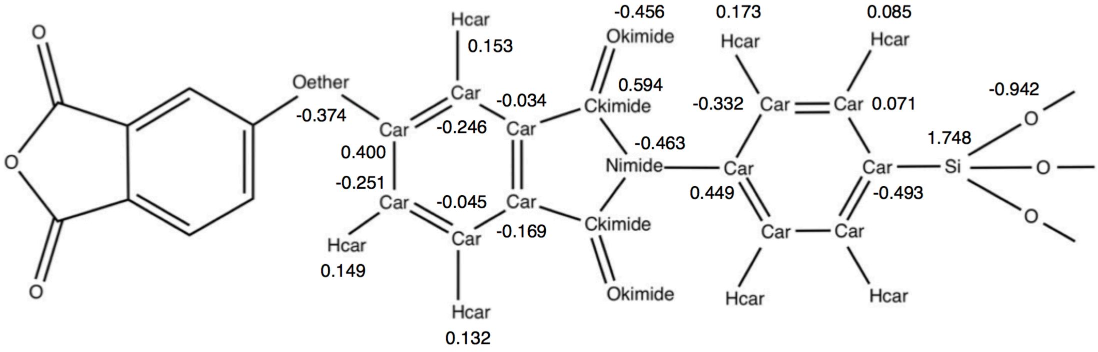

poly*ortho*OAPS-ODPA

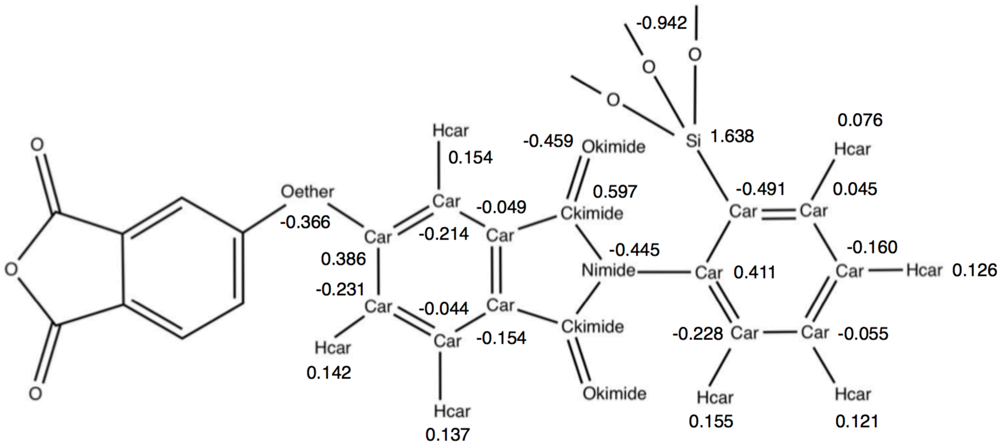

Fig. S1 The partial charges q_i/e for all OAPS-based and dianhydride-based molecules

2) THE EXPERIMENTAL PROCEDURE

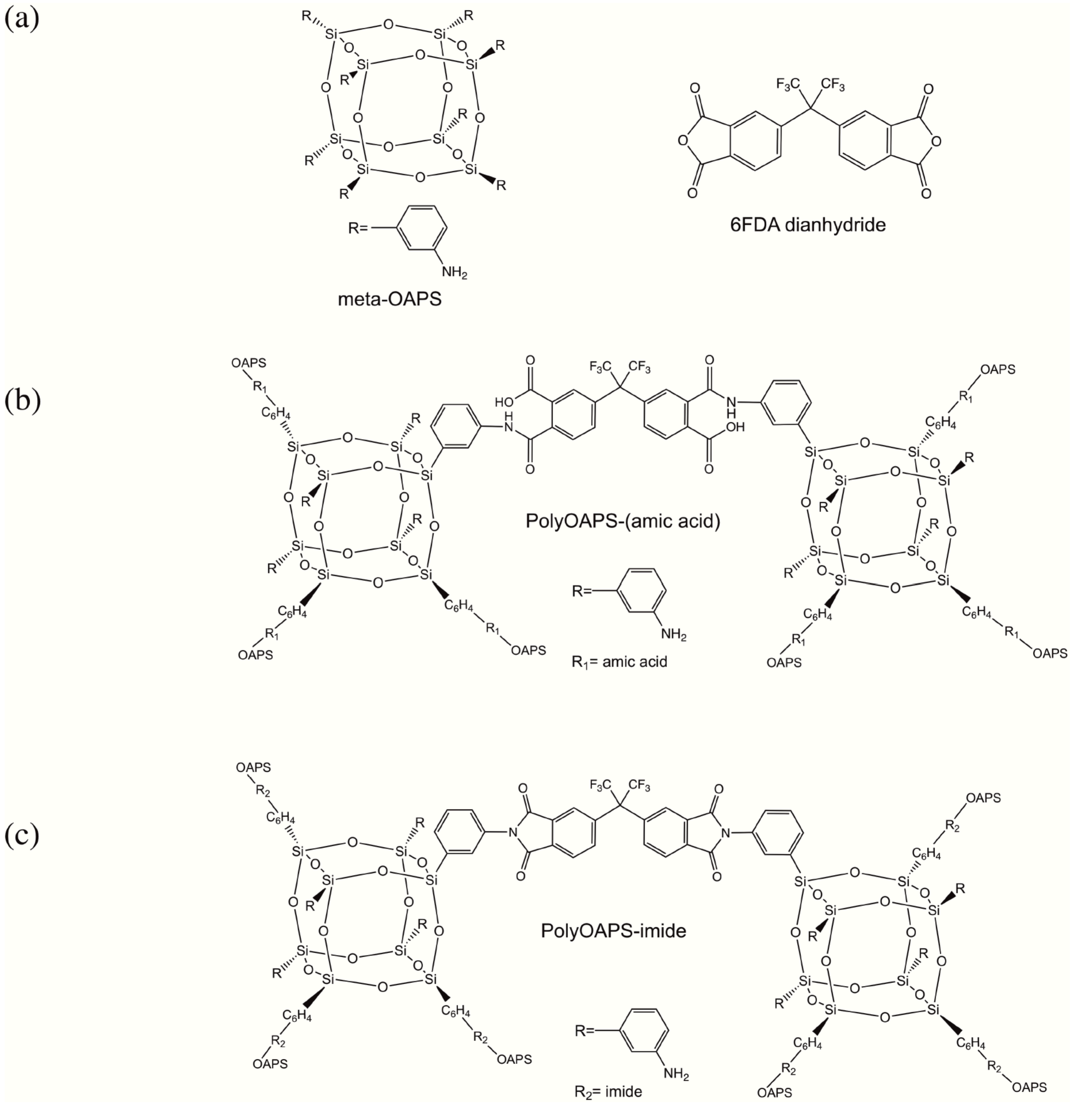

Fig. S2 Schematic representation of the synthesis of the hyper-cross-linked polyOAPS-imide networks based on *meta*OAPS and 6FDA. **(a)** the reactants, **(b)** the interfacial polycondensation and **(c)** the thermal imidization carried out at 300°C.

3) THE TWO-STAGE VERSUS DIRECT CONVERSION FROM UN-CROSS-LINKED DIANHYDRIDE:POSS MIXTURES TO CROSS-LINKED POLYPOSS-IMIDES

In our previous work using the aliphatic POSS precursor and the 6FDA and PMDA dianhydrides,[1,2,18] the initial polymerization step, which leads to the formation of a polyPOSS-(amic acid), was explicitly simulated before relaxing the resulting system and subsequently performing the imidization step at 300°C. Although this mimicked very closely the experimental procedure, it introduced significant extra complexity and expenditure of computer time even though the connectivity of the final network is defined once the initial transformation to the polyPOSS-(amic acid) is made. To assess whether the intermediate amic acid step could be avoided, the three original samples containing 3:1 mixtures of dianhydride:POSS were transformed directly to the polyPOSS-imide form using basically the same method to that already described.[1,2] The only difference was that, at each reaction step, the transformation was directly made to the imide form with the concomitant elimination of one H_2O molecule per imidization. The subsequent relaxations of the polyPOSS-imide densities at 300°C and 1 bar are shown in Fig. S3.

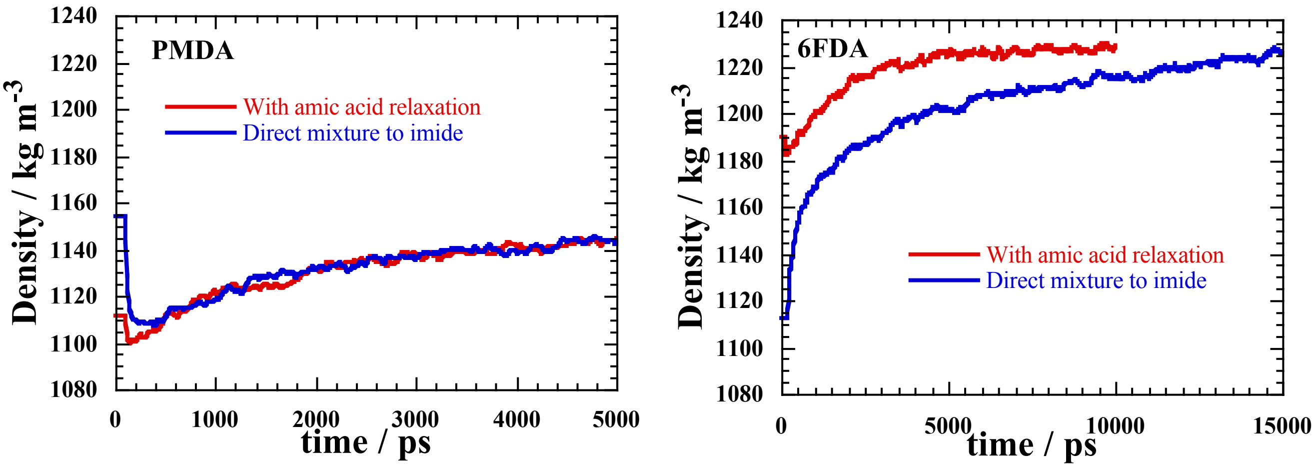

Fig. S3. Density relaxation at 300°C for the (**left**) polyPOSS-PMDA and (**right**) polyPOSS-6FDA imides following: (i) an initial polymerization to the amic acid form, relaxation of the amic acid and then conversion to the polyimide form and (ii) a direct conversion of the mixture to the polyimide form.

As can be seen from Fig. S3, very similar results were obtained for the relaxed density. Checks of the various energies confirmed the viability of making the direct conversion to the imide form. The connectivity statistics were also examined and these are given in Table S4. The change from a 2-stage process to a direct conversion influences particularly the time it takes to perform the required number of reactions with the elimination of H_2O in the direct conversion favourising shorter reaction times. Otherwise the connection statistics remain very similar with average inter-POSS connectivities between 3.1 and 3.2.

Table S4. Reaction statistics for mixtures of 648 dianhydride and 216 POSS molecules, i.e. a 3:1 ratio, and after 432 reactions, i.e. a 2:1 ratio of imide groups to POSS arms using R_{min} = 6 Å. The transformation was either (i) done in two stages: mixture to amic acid followed by relaxation and then amic acid to imide, as reported previously,[1,2] or (ii) by direct mixture-to-imide reactions. In each case averages were taken over three samples.

	(i) 2-stage transformation	**(ii) Direct transformation**	**(i) 2-stage transformation**	**(ii) Direct transformation**
Structure	**polyPOSS-6FDA**		**polyPOSS-PMDA**	
No. of links	432	432	432	432
No. of links per POSS	4	4	4	4
No. of intraPOSS links	61.0	72.7	71.0	73.3
% of intraPOSS links	14.1	16.8	16.4	17.0
No. of INTRA arms/POSS	0.56	0.67	0.66	0.68
No. of INTER arms/POSS	3.44	3.33	3.34	3.32
No. diff. POSS linked to a POSS	3.18	3.10	3.11	3.08
% of POSS having:-				
0 links	0.8	0.9	0.5	0.6
1 link	4.6	4.6	2.9	4.9
2 links	12.0	11.6	12.7	11.6
3 links	18.4	19.9	21.5	19.1
4 links	26.9	25.3	25.5	25.5
5 links	20.8	21.1	20.8	20.7
6 links	11.4	11.0	12.2	14.2
7 links	4.6	4.6	3.9	3.1
8 links	0.5	0.9	0.2	0.3
% of atoms in continuous network	98.8	98.4	98.8	99.1
No. molecules after reactions	3.67	5	4	3.33
Time to react / ps	6964	1570	851	383

4) CHOICE OF THE LIMIT CRITERION FOR $\mathbf{R_{min}}$

The limit criterion, which controls which dianhydrides are selected for cross-linking, is based on the mixtures radial distribution functions g(*r*) between the OAPS nitrogen N and the dianhydride ketone carbons C_{ket}. Only those dianhydrides having the sum, R_{min}, of their shortest $C_{ket}\cdots N$ distances at either end being less than the limit criterion are reacted. The $C_{ket}\cdots N$ g(*r*) are displayed in Fig. S4. Unlike the *para*OAPS and *meta*OAPS isomers, there are relatively few cases in the dianhydride:*ortho*OAPS mixture, where the $C_{ket}\cdots N$ distances are less than 3 Å. Using a limit criterion of 6 Å (as was done before for polyPOSS-PMDA)[2] would thus exclude all connections via the *ortho*-substituted OAPS. Without any experimental information suggesting that imide bridges between *ortho*-substituted arms are unlikely, it was decided to change the criterion for reactions to $R_{min} \leq 7$ Å. This was previously tested for polyPOSS-6FDA networks and was shown to give identical results to the initial R_{min} of 6 Å.[1]

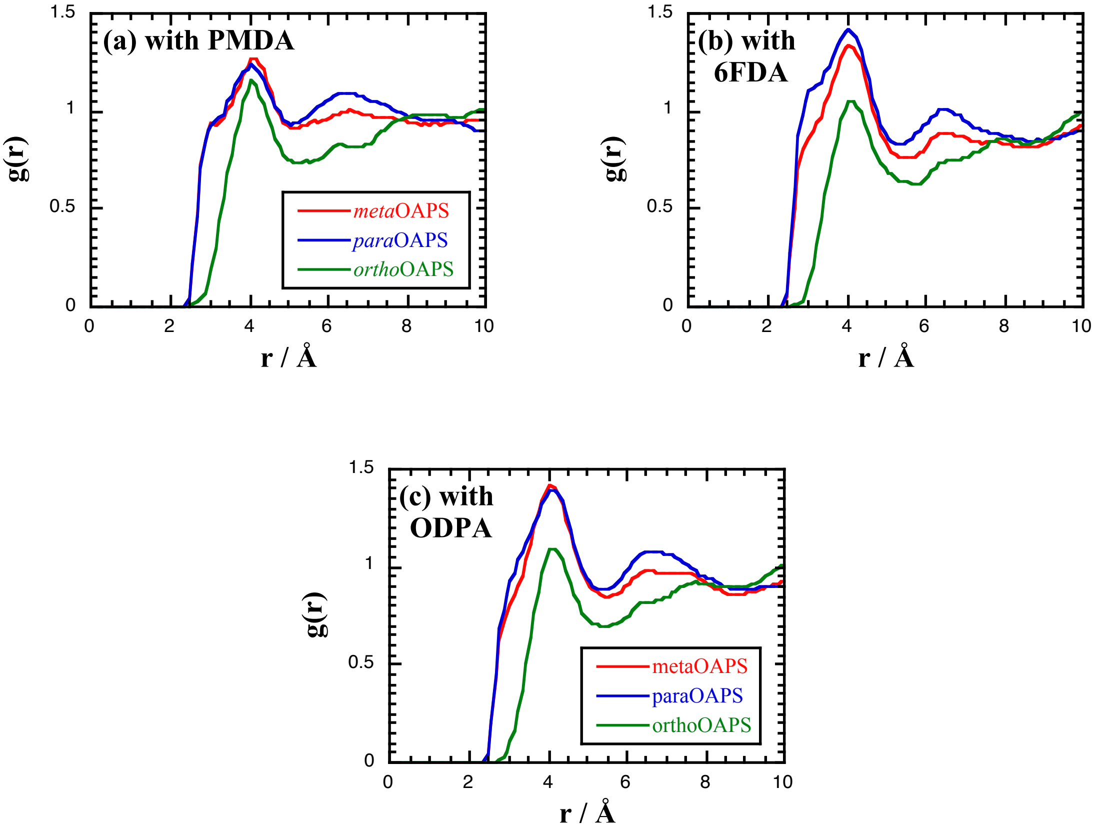

Fig. S4. Radial distribution functions g(*r*) in the mixtures between the dianhydride C_{ket} and the OAPS N as a function of the nature of the dianhydride and the OAPS isomer.

5) SIMULATION TIMES FOR THE CROSS-LINKING PROCEDURE

As explained in the text, the mixtures were first cross-linked up to 432 reactions, *i.e.* to the same average connectivity of four links per cage. They were further allowed to react until completion, *i.e.* until there were either no more possible reactions or when further reactions led to steric hindrances that could not be relaxed out sufficiently to allow the MD to restart. While both approaches led to continuous networks, the time needed to complete all the reactions was significantly increased when aiming for completion. This is displayed in Fig. S5 for the systems linked with the PMDA and ODPA dianhydrides.

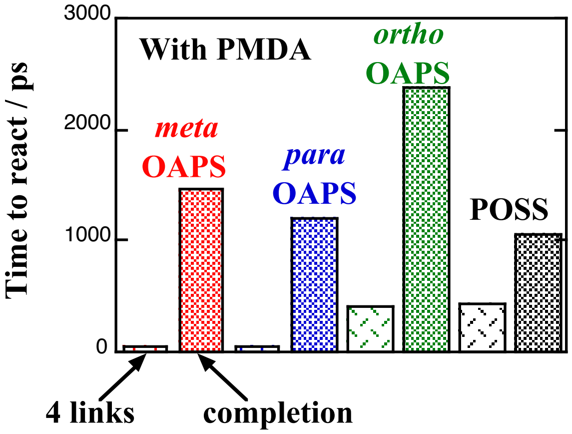

(a)

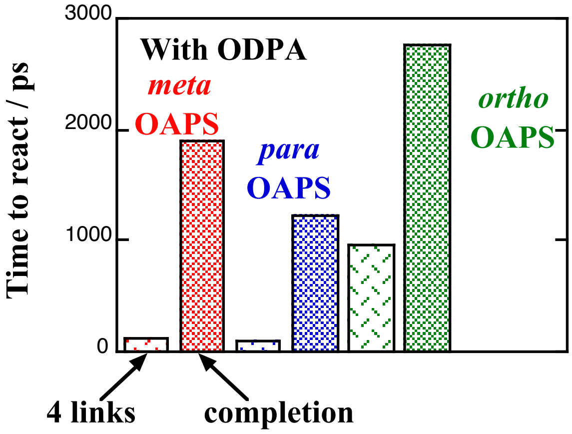

(b)

Fig. S5 Simulation times of the cross-linking procedure which are needed to reach an average connectivity of 4 links per cage (left bars) compared to those needed to go to completion (right bars) for **(a)** the polyOAPS-PMDA and polyPOSS-PMDA and (**b)** the polyOAPS-ODPA systems.

6) RELAXATION RUNS AT 300°C AND ENERGIES

Following the completion of the cross-linking procedure, the twenty-two networks were run under *NPT* conditions at 300°C up to 20000 ps in order to stabilize their densities and energies. Fig. S6 displays the relaxation of the poly*para*OAPS-6FDA system. It is clear that it can be considered as being properly relaxed within this timescale. The analyses were carried out on the last 5000 ps of these runs.

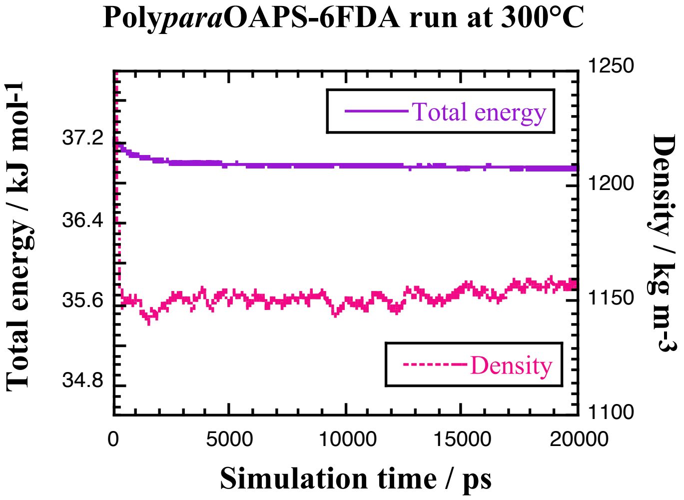

Fig. S6. Evolution of the total energy (left axis) and the density (right axis) upon relaxation at 300°C for the poly*para*OAPS-6FDA model network.

The relaxed densities are given in Table 3 (main text) and the components of the energies at 300°C are presented in Table S5 hereafter.

Table S5. Energies in kJ mol^{-1} (of atoms) at 300°C for the 22 polyOAPS-imides and polyPOSS-imides under study. The various terms correspond to Eqs B, C, D, E and G. The maximum standard error is 0.01 kJ mol^{-1}.

Property	***meta*** **OAPS** + **PMDA**	***para*** **OAPS** + **PMDA**	***ortho*** **OAPS** + **PMDA**	**POSS** + **PMDA**	***meta*** **OAPS** + **6FDA**	***para*** **OAPS** + **6FDA**	***ortho*** **OAPS** + **6FDA**	**POSS** + **6FDA**	***meta*** **OAPS** + **ODPA**	***para*** **OAPS** + **ODPA**	***ortho*** **OAPS** + **ODPA**
	Average connectivity of 4 links per cage										
$<U_{bend}>$	2.92	3.05	3.82	3.56	2.77	2.93	3.09	3.36	2.63	2.81	2.94
$<U_{tors}>$	2.19	2.38	3.55	1.12	1.54	1.81	2.21	0.91	1.75	2.15	2.45
$<U_{oop}>$	0.67	0.62	0.84	0.33	0.44	0.47	0.48	0.26	0.49	0.53	0.52
$<U_{vdw}>$	-1.49	-1.13	-1.86	-1.52	-1.53	-1.37	-1.61	-1.44	-1.75	-1.51	-1.87
$<U_{coul}>$	75.78	50.30	28.36	57.56	56.93	34.30	14.93	42.32	63.06	39.47	20.24
	Connectivity reactions carried out until completion										
$<U_{bend}>$	3.46	3.72	4.45	3.83	3.01	3.20	3.25	3.50	2.97	3.24	3.19
$<U_{tors}>$	2.60	3.03	4.01	1.25	1.58	1.94	2.24	0.97	1.87	2.41	2.55
$<U_{oop}>$	0.81	0.78	0.97	0.40	0.46	0.50	0.50	0.29	0.53	0.59	0.56
$<U_{vdw}>$	-1.45	-1.09	-1.96	-1.59	-1.49	-1.35	-1.61	-1.49	-1.72	-1.55	-1.94
$<U_{coul}>$	70.85	45.06	28.93	53.76	51.67	29.41	13.98	37.96	56.28	32.97	19.42

7) INTERCAGE VS INTRACAGE LINKS

The average number of inter- and intra- links are compared in Fig. S7 for all 22 structures screened. They are also displayed as stack columns in Fig. 7 (main text).

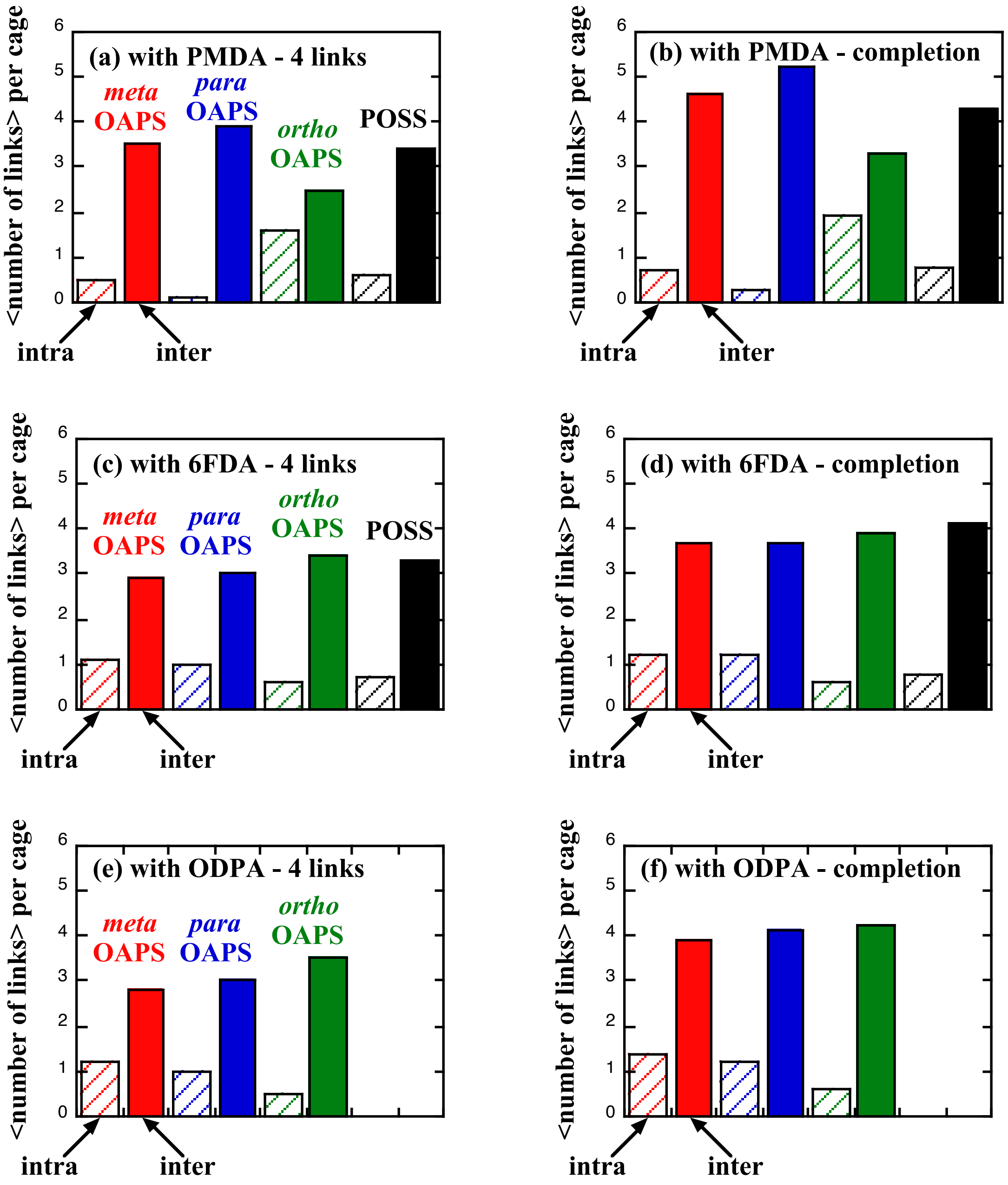

Fig. S7 Average number of intraOAPS or intraPOSS links (left bars, stripes) and interOAPS or interPOSS links (right bars, full colour) in all the networks generated. (**a-b**) refer to the PMDA-based, (**c-d**) to the 6FDA-based and (**e-f**) to the ODPA-based networks.

8) INTERCAGE SINGLE-LINKS VS DOUBLE-LINKS

Fig. S8 shows the percentages of cages having one intercage double-link (*i.e.* with two different arms of another cage) and all its other links being intercage single-links for the 22 structures screened. They are inversely proportional to the number of intracage links and represent ~10-20% of the cages.

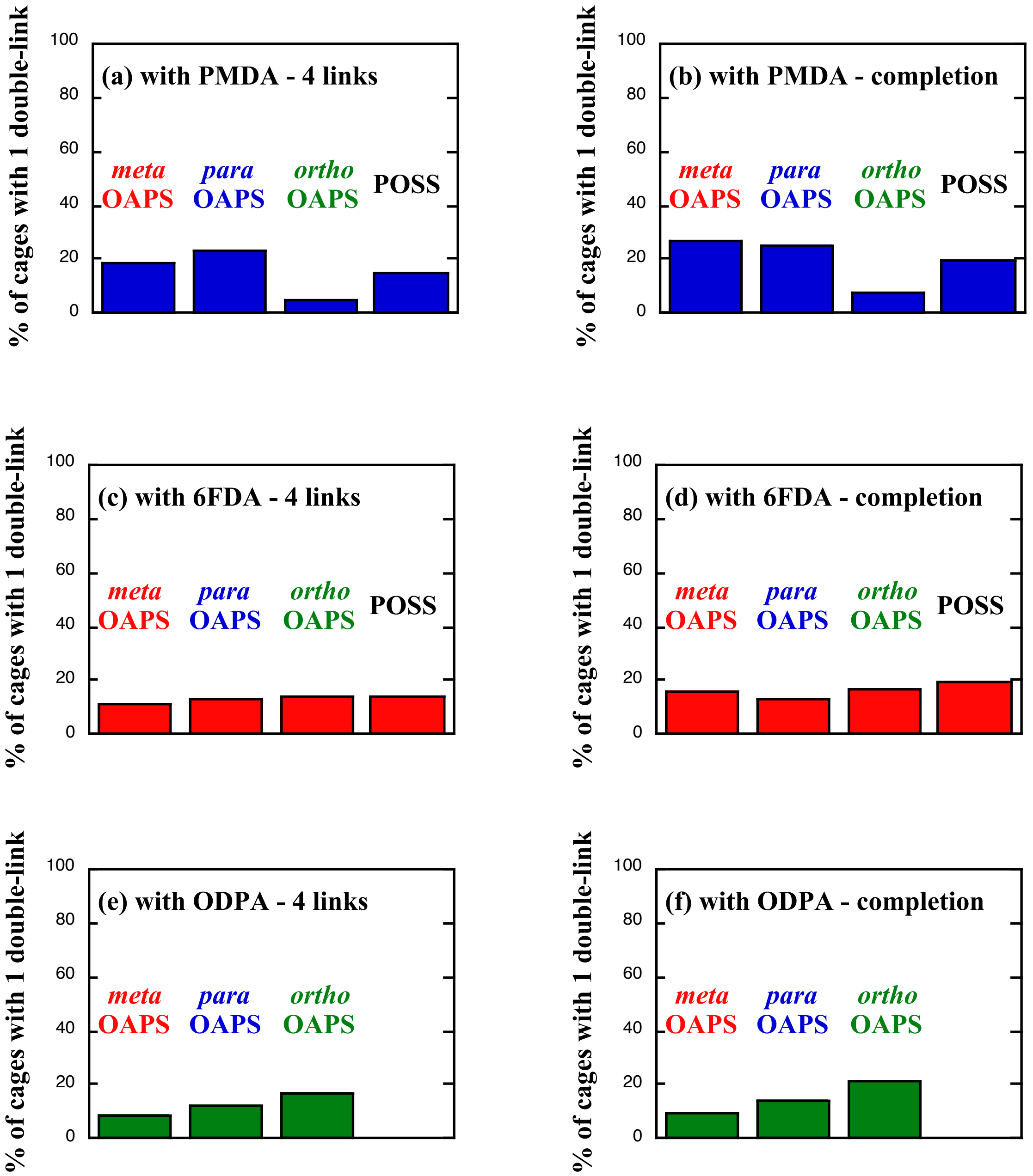

Fig. S8 Percentages of cages having one interOAPS or interPOSS double-link and all their other links being interOAPS or interPOSS single-links.

9) DEFORMATION UPON ISOTROPIC DILATION AT 300°C

Fig. S9 separates the resistance to dilation of the inorganic part of the linker (left Figures), from that of the organic part of the linker (right Figures), for the 11 networks with the average connectivity of 4 links *per* cage.

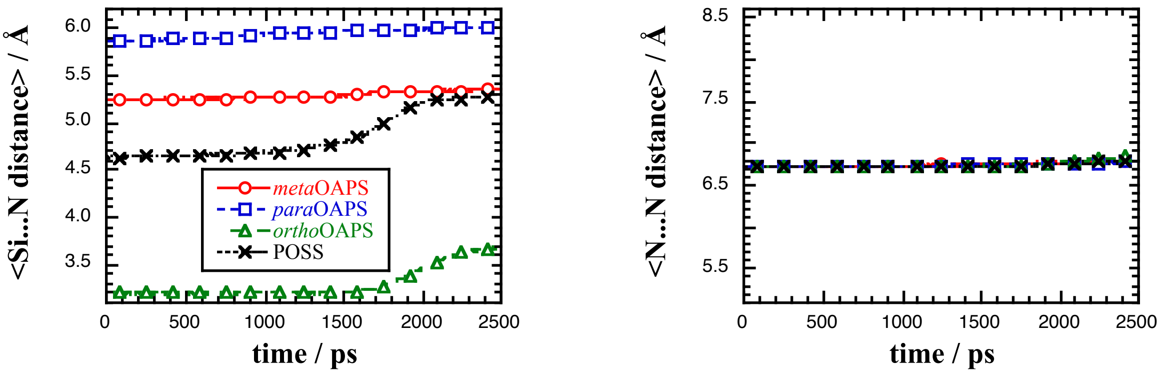
(a) with PMDA - inorganic linker

(b) with PMDA - organic linker

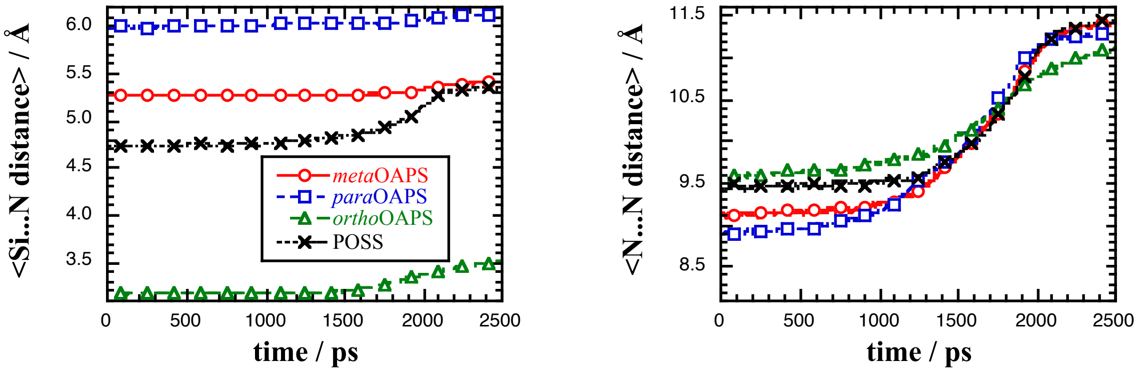
(c) with 6FDA - inorganic linker

(d) with 6FDA - organic linker

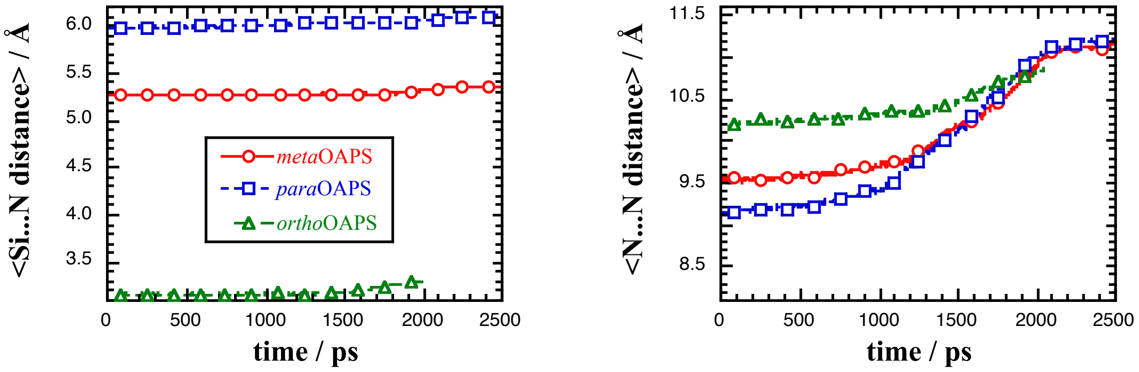
(e) with ODPA - inorganic linker

(f) with ODPA - organic linker

Fig. S9 Time evolutions of the average Si...N distance representing the inorganic part of the linker (left Figures), and the average N...N distance representing the organic part of the linker (right Figures), for all the networks whose average connectivity is 4 links *per* cage.

10) RELAXATION RUNS AT 400°C AND ENERGIES

The polyOAPS-imide networks with the connectivity carried out until completion were heated from 300°C to 400°C and run under *NPT* conditions up to 5000 ps in order to stabilize their densities and energies. Fig. S10 displays the relaxation of the poly*para*OAPS-6FDA system. It is clear that it relaxes very rapidly within this timescale.

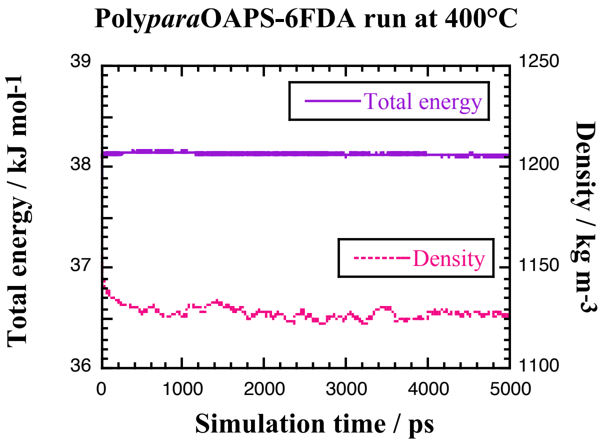
Poly*para*OAPS-6FDA run at 400°C

Fig. S10. Evolution of the total energy (left axis) and the density (right axis) upon relaxation at 400°C for the poly*para*OAPS-6FDA model network.

The relaxed densities are given in Table 7 (main text) and the components of the energies at 400°C are presented in Table S6 hereafter.

Table S6. Energies in kJ mol^{-1} (of atoms) at 400°C for the 9 polyOAPS-imides with the connectivity carried out until completion. The various terms correspond to Eqs B, C, D, E and G. The maximum standard error is 0.01 kJ mol^{-1}.

Property	***meta*** **OAPS + PMDA**	***para*** **OAPS + PMDA**	***ortho*** **OAPS + PMDA**	***meta*** **OAPS + 6FDA**	***para*** **OAPS + 6FDA**	***ortho*** **OAPS + 6FDA**	***meta*** **OAPS + ODPA**	***para*** **OAPS + ODPA**	***ortho*** **OAPS + ODPA**
$<U_{bend}>$	3.68	3.95	4.69	3.25	3.44	3.51	3.17	3.44	3.41
$<U_{tors}>$	2.70	3.12	4.13	1.68	2.04	2.36	1.98	2.50	2.67
$<U_{oop}>$	0.90	0.86	1.06	0.53	0.57	0.57	0.62	0.67	0.64
$<U_{vdw}>$	-1.32	-0.95	-1.85	-1.34	-1.20	-1.49	-1.57	-1.39	-1.81
$<U_{coul}>$	70.88	45.10	28.95	51.70	29.44	14.00	56.31	33.01	19.45

References

1. S. Neyertz, D. Brown, M. J. T. Raaijmakers and N. E. Benes, *Phys. Chem. Chem. Phys.*, 2016, **18**, 28688-28703.
2. S. Neyertz, D. Brown, M. J. T. Raaijmakers and N. E. Benes, *Comp. Mater. Sci.*, 2016, **117**, 338-353.
3. D. Brown, *The gmq User Manual Version 6: available at* http://www.lmops.univ-savoie.fr/brown/gmq.html, 2021.
4. K. D. Hammonds and J.-P. Ryckaert, *Comput. Phys. Commun.*, 1991, **62**, 336-351.
5. G. Ciccotti, M. Ferrario and J. P. Ryckaert, *Mol. Phys.*, 1982, **47**, 1253-1264.
6. M. P. Allen and D. J. Tildesley, *Computer Simulation of Liquids*, Clarendon Press, Oxford, UK, 1987.
7. P. P. Ewald, *Ann. Phys.*, 1921, **369**, 253-287.
8. W. Smith, *Comput. Phys. Commun.*, 1992, **67**, 392-406.
9. D. Fincham, *Mol. Simul.*, 1994, **13**, 1-19.
10. M. J. Frisch, G. W. Trucks, H. B. Schlegel, G. E. Scuseria, M. A. Robb, J. R. Cheeseman, G. Scalmani, V. Barone, B. Mennucci, G. A. Petersson, H. Nakatsuji, M. Caricato, X. Li, H. P. Hratchian, A. F. Izmaylov, J. Bloino, G. Zheng, J. L. Sonnenberg, M. Hada, M. Ehara, K. Toyota, R. Fukuda, J. Hasegawa, M. Ishida, T. Nakajima, Y. Honda, O. Kitao, H. Nakai, T. Vreven, J. A. Montgomery Jr., J. E. Peralta, F. Ogliaro, M. Bearpark, J. J. Heyd, E. Brothers, K. N. Kudin, V. N. Staroverov, R. Kobayashi, J. Normand, K. Raghavachari, A. Rendell, J. C. Burant, S. S. Iyengar, J. Tomasi, M. Cossi, N. Rega, J. M. Millam, M. Klene, J. E. Knox, J. B. Cross, V. Bakken, C. Adamo, J. Jaramillo, R. Gomperts, R. E. Stratmann, O. Yazyev, A. J. Austin, R. Cammi, C. Pomelli, J. W. Ochterski, R. L. Martin, K. Morokuma, V. G. Zakrzewski, G. A. Voth, P. Salvador, J. J. Dannenberg, S. Dapprich, A. D. Daniels, O. Farkas, J. B. Foresman, J. V. Ortiz, J. Cioslowski and D. J. Fox, *Journal*, 2009.
11. U. C. Singh and P. A. Kollman, *J. Comput. Chem.*, 1984, **5**, 129-145.
12. B. H. Besler, K. M. Merz Jr. and P. A. Kollman, *J. Comput. Chem.*, 1990, **11**, 431-439.
13. M. Clark, R. D. Cramer III and N. Van Opdenbosch, *J. Comput. Chem.*, 1989, **10**, 982-1012.
14. A. Striolo, C. McCabe and P. T. Cummings, *Macromolecules*, 2005, **38**, 8950-8959.
15. Z. A. Makrodimitri, R. Dohrn and I. G. Economou, *Macromolecules*, 2007, **40**, 1720-1729.
16. J. J. Freire, I. F. Piérola and A. Horta, *Macromolecules*, 1996, **29**, 5143-5148.
17. Y. Yani and M. H. Lamm, *Polymer*, 2009, **50**, 1324-1332.
18. D. Brown, S. Neyertz, M. J. T. Raaijmakers and N. E. Benes, *J. Membr. Sci.*, 2019, **577**, 113-119.